Energy, economic and environmental benefits of Demand Response for improving building energy flexibility

Enrico Dal Cin[1*], *Sergio* Rech[2], and *Marianna* Benetti[3]

[1]University of Padova, Industrial Engineering Department, 35121 Padova PD, Italy
[2]University of Padova, Energy Economics and Technology Institute "Giorgio Levi Cases", 35121 Padova PD, Italy
[3]Veil Energy S.r.l. SB, 39100 Bolzano BZ, Italy

Abstract. The increasing penetration of intermittent renewable sources in power generation at local and building-level poses growing issues in balancing generation and demand. To avoid imbalances, it is therefore necessary to ensure adequate levels of flexibility in the building energy system. This can be done both on the generation side, through the coupling of different energy carriers (cogeneration, power-to-heat solutions) and/or the integration of storage systems, and on the demand side, through smart "demand response" programs. This paper considers a tourist facility located in central Germany as a case study to evaluate the energy, economic and environmental benefits that can be obtained from the application of appropriate demand response strategies. The electrical demand data of the facility are monitored at both aggregate and individual load levels and made available by means of a cloud platform. The facility includes two stationary combined heat and power internal combustion engines powered by natural gas and a photovoltaic system. The results show how, thanks to appropriate load management, it is possible, on the one hand, to increase the self-consumption of PV-generated energy and, on the other hand, to keep more constant the load of the engines, which can therefore operate with better efficiencies. This results in both a reduction in energy expenses and a decrease in carbon dioxide emissions attributable to the building.

1 Introduction

The transition to a sustainable energy system necessitates increased generation of energy from renewable sources, more efficient but declining use of fossil fuels, and increasing electrification of end uses [1]. At the European level, the buildings sector is responsible for about 40% of final energy consumption [2] and will therefore be crucial in meeting the goal of achieving climate neutrality by 2050 [3].

However, the increasing penetration of non-programmable renewable sources (mainly photovoltaic and wind) in local and building-level power generation poses increasing problems of balancing generation and demand, which may negatively impact the stability of

* Corresponding author: enrico.dalcin@phd.unipd.it

the power grid [4]. To avoid imbalances, it is therefore necessary to ensure adequate levels of flexibility in the building energy system. This can be done either on the generation side, through the coupling of different energy carriers (cogeneration, power-to-heat solutions) and/or the integration of storage systems, or on the demand side, through smart "demand response" (DR) programs [5].

DR is defined by the U.S. Department of Energy as "*changes in electric usage by end-use customers from their normal consumption patterns in response to changes in the price of electricity over time, or to incentive payments designed to induce lower electricity use at times of high wholesale market prices or when system reliability is jeopardized*" [6]. Direct or indirect control of electrical loads in addition to increasing the stability of the electrical system can significantly reduce its costs [7]. In fact, a better balance between demand and generation at the local level makes it possible to postpone or reduce investment in capital-intensive electricity infrastructure [8].

However, the positive impacts of DR are struggling to emerge due to social, technological, economic, and legislative barriers that limit its diffusion [9]. A turning point in favour of using efficient DR strategies has been the transition to a deregulated and liberalized electricity market [10]. DR based on time-varying electricity prices (time-of-use tariffs, day-ahead and real-time markets) has proven to be the most efficient and easily implemented method at the local and building level for demand management and balancing with available generation [11]. Given the flexibility of demand versus price, end customers are driven to reduce consumption during peak periods and increase consumption during off-peak periods or periods with high energy availability [12]. This also promotes the penetration of distributed generation from intermittent renewable sources by reducing excess generation [13].

In summary, an effective and applicable DR strategy must be beneficial to both the system and the user by setting three objectives of energy, environmental, and economic nature, respectively [14]:

- Minimizing the unbalance between demand and generation,
- Maximizing the use of renewable sources at the local level,
- Maximizing the savings achievable by participants.

In the literature, DR has frequently been treated in the form of an optimization problem, in which the demand curve must be modified respecting certain constraints in order to minimize or maximize one or more objective functions (see, for example, the objectives above). The most widely used optimization techniques are linear programming (LP) and mixed integer linear programming (MILP), given their availability as commercial software, their ability to handle a large number of decision variables, their capability to find the global optimum of the problem and their computational efficiency [15]. The applications are wide-ranging, but often refer to very specific case studies and areas of research such as, for example, the problem of expanding the power grid and generating capacity [16], the frequency control of the power grid [17], the stability of an isolated microgrid [18].

Some Authors of the work proposed here have already dealt with the DR problem within studies on renewable energy communities [19, 20], although the focus has been primarily on optimizing the design and/or operation of generation and storage units rather than on the actual characterization of the demand curve, which is modelled at the aggregate level.

Finally, some studies have dealt with the application of DR at the building level for automatic load management using MILP algorithms [21] or neural networks [22]. In these studies, however, load curves are obtained from simulation of the modelled equipment, while measured consumption data are missing.

In contrast, the work proposed here is based on consumption data collected from measurements taken at a tourist facility located in Hausen, Germany (north-western Bavaria) during 2023. Each electrical load/group of loads in the building (lighting, appliances,

swimming pool equipment, cooling and ventilation units...) is equipped with a multifunction electronic measurement digital unit, which makes available measured values of key electrical quantities, including active power consumed/produced, to a real-time monitoring and management cloud platform [23]. The building is also equipped with a photovoltaic (PV) plant and two stationary internal combustion engines (ICEs) operating in combined heat and power mode.

In the literature, electrical loads are often categorized as fixed loads (nonadjustable), shiftable loads (the use of which can be postponed or brought forward within the day while keeping the integral of consumption fixed), curtailable loads (the consumption of which can be reduced in precise time intervals), and loads that can be directly controlled by changing operating conditions (e.g., the operation of a chiller can be changed by changing the temperature set point) [24]. In this paper, all monitored loads are categorized into two groups, fixed loads and shiftable loads. On the former there is no room for intervention through DR, while the latter can be "moved" to different time slots within the day according to predefined levels of flexibility.

The objective of the study is to find the optimal strategy for managing shiftable loads and generation plants that minimizes daily operating costs to meet the building's overall electrical demand. It will also be seen how cost minimization leads to benefits in terms of increased use of local renewable sources (solar) and reduction of peak demand and generation witnessed by the power grid. To this end, a detailed optimization model is built considering both continuous and binary decision variables (MILP model).

The analyses have been conducted on representative seasonal days (typical days) considering two different tariff plans for purchasing electricity from the grid. In the first case, purchase is at a fixed constant price, while in the second case a time-of-use (TOU) tariff is considered. Different levels of "flexibility" of shiftable loads have also been considered, assuming different levels of user involvement in applying the indications provided by the DR algorithm. In the worst case (zero flexibility), the user does not accept any of the proposed load changes, leaving the overall demand curve unchanged. In the best case (maximum flexibility), the user makes itself available to handle all shiftable loads as proposed by the DR model. In the intermediate cases, instead, it makes itself available to act only on a specified portion of the overall shiftable load.

2 Case study

Fig. 1 depicts the system considered in this paper. The system includes the building of a tourist facility located in Hausen, Germany (northwestern Bavaria), a 500 kWp photovoltaic plant (annual producibility of 705 MWh), and two natural gas-fuelled internal combustion engines of 200 kW (ICE_1) and 100 kW (ICE_2) of rated electrical power. There are a total of 40 electrical loads, 11 of which have been identified as shiftable loads. The latter include household appliances (industrial washing machines and dishwashers), air conditioning systems, circulation pumps, and swimming pool auxiliaries. Measurements are performed by multifunction electronic measurement digital units installed in the electrical panels of the above-mentioned electrical loads. These devices comply with EN/IEC 6155712 and the maximum error on active power is 1% (measuring instruments belong to class 0.5 or class 1). All measured data are collected via Modbus/TCP protocol by a central router that sends them to a monitoring and management cloud platform [23]. Finally, the platform historizes data at an average rate of 10s, and processes them to respond with control signals toward ICEs and displaceable loads.

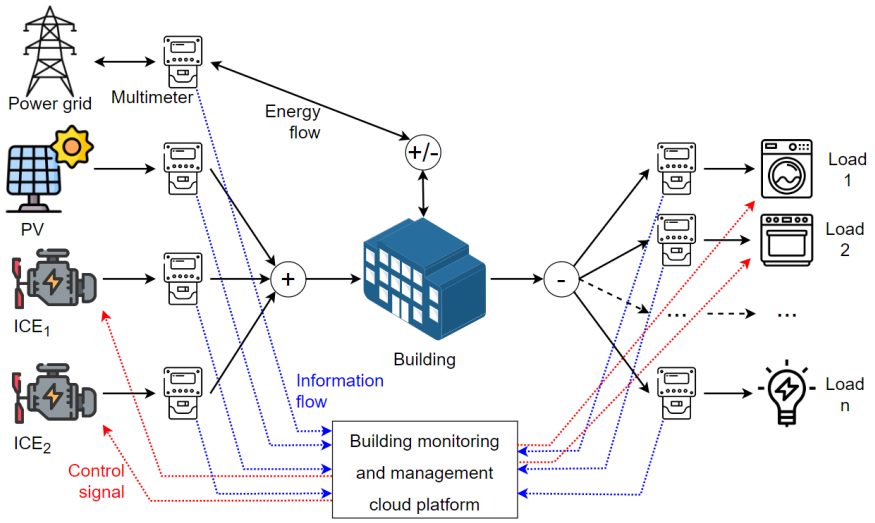

Fig. 1. Representative diagram of the case study considered.

2.1 Model input data

Data of electric power consumed by various loads are recorded at varying cadences depending on the frequency and magnitude of load variation. The interval between two consecutive measurements is between 10 seconds and 1 minute. The resulting amount of data is far greater than that required for the purposes of this study, which does not require such precise temporal resolution. Consumption data are therefore aggregated into four seasonal typical days with hourly discretization (winter is considered from December to February, spring from March to May, summer from June to July, and autumn from September to November). Aggregation into typical days is achieved by the time-weighted average of all power readings at a given time of day in a given season weighted with the elapsed time interval until the next reading (if the meter does not detect change in power, it does not record new readings). The total electricity consumption is 3415 kWh for the typical winter day, 3890 kWh for the spring day, 5007 kWh for the summer day, and 5323 kWh for the autumn day. Of these, shiftable loads count for 1181 kWh (35%) in the winter typical day, 1363 kWh (35%) in the spring typical day, 2683 kWh (54%) in the summer typical day, and 2801 kWh (53%) in the autumn typical day.

The PV modules are oriented to the south and tilted 40° from the horizontal plane. The global solar radiation data on the tilted plane needed for calculating the generated power are available on an hourly basis for several years [25] and are aggregated into typical seasonal days in the same way as power measurements. Electricity production from PV is 1130 kWh for the typical winter day, 2517 kWh for the spring day, 2705 kWh for the summer day, and 1373 kWh for the autumn day.

The cost of natural gas burned by the stationary engines is assumed constant and equal to 60 €/MWh considering the lower heating value [26], while the direct carbon dioxide (CO_2) emissions associated with combustion are 197 kg/MWh. Regarding electricity taken from the grid, two possible alternative tariff plans are considered (Fig. 2):

- Fixed tariff of 290 €/MWh,
- Time-of-use (TOU) tariff variable over three bands [27].

The CO_2 emission factor associated with energy taken from the grid is set at 371 kg/MWh [28]. Electricity sold to the grid is remunerated at a fixed rate of 50 €/kWh corresponding to the average annual value of the price on the wholesale market [29].

Table 1 reports data on the operation of stationary engines [30, 31].

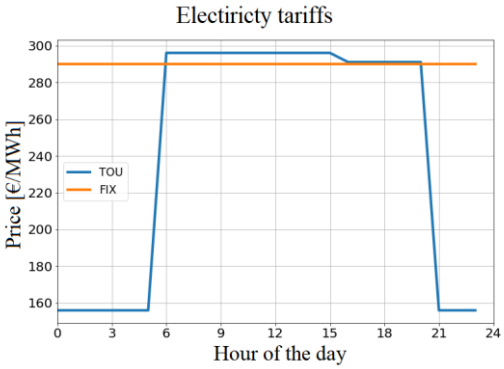

Fig. 2. Tariffs related to electricity withdrawal from the grid: fixed (FIX) and variable (TOU).

Table 1. Operating data of the two stationary internal combustion engines.

Quantity	Unit	ICE_1	ICE_2
Electrical efficiency at full load	%	37	34
Electrical efficiency at minimum load	%	30	27
Minimum load-full load ratio	%	70	70
Maximum number of daily on/offs	-	2	2
Operation and maintenance cost	€/MWh_{el}	5.4	5.4

3 Optimization model

The optimization problem consists in minimizing the daily operating costs of meeting the electrical demand of the system shown in Figure 1 by considering the possibility of changing the consumption pattern of "shiftable" loads. This problem is solved by a rigorous procedure based on a physical model of the system [32].

In order to limit computational time, both the objective function and the model constraints are expressed as linear relations only. In addition, the decision variables are partly continuous and partly binary. Thus, the problem is configured as MILP.

3.1 Decision variables

Table 2 reports the decision variables of the model, defined for each hour h of the typical day under consideration. They include the electrical power generated by the engines, their on/off status (binary variables), the power imported and exported with respect to the grid, and the aggregate electrical demand of the shiftable loads downstream of the DR application. Additional auxiliary decision variables are omitted here.

Table 2. Decision variables.

Name of the variable	Symbol	Unit	Type
Generated power, ICE1	P_{ICE1}	kW	Continuous
On/off status, ICE1	δ_{ICE1}	-	Binary
Generated power, ICE2	P_{ICE2}	kW	Continuous
On/off status, ICE2	δ_{ICE2}	-	Binary
Power imported from the grid	P_{imp}	kW	Continuous
Power injected into the grid	P_{exp}	kW	Continuous
Power consumed, shiftable loads	D_{DR}	kW	Continuous

3.2 Constraints

Equation (1) reports the electric power balance holding in each hour of the day, where D_{fix} is the aggregated demand of fixed loads in kW and P_{PV} is the power generation of the PV plant in kW as calculated in Equation(2), where, in turn, Cap_{PV}=500kW$_p$ is the rated power of the plant, I_{ref}=1000 W/m^2 is the solar irradiance in standard peak conditions and I_h is the actual irradiance during the hour h in W/m^2.

$$D_{fix,h} + D_{DR,h} + P_{exp,h} = P_{PV,h} + P_{MCI_1,h} + P_{MCI_2,h} + P_{imp,h} \quad (1)$$

$$P_{PV,h} = Cap_{PV} \frac{I_h}{I_{ref}} \quad (2)$$

Note that, since historical ambient temperature measurements are not available, the influence of outdoor temperature on PV module efficiency is not considered. The temperature considered is the standard reference temperature, which is 25°C. Considering that the average annual temperature at the analysed location is about 9°C, the estimates made can be considered conservative. Assuming that ambient temperature measurements were available, it would be possible to account for the effect of temperature on efficiency by means of a correction factor that, depending only on input data, would not affect the linearity of the model.

The characteristic equation for the operation of ICEs describes the relationship between specific fuel consumption and electrical power generation. This relationship has been linearized between the point of operation at rated load (100%) and the point of operation at minimum part load (70%) and is therefore described by a pair of values – angle coefficient (m) and intercept (q) – for each engine. These values can be calculated from the efficiencies given in Table 1. Equation (3) calculates the fuel consumption (C_{ICE}) as a function of the power generated by generic engine i.

$$C_{ICE_i,h} = P_{ICE_i,h} m_i + q_i \quad (3)$$

The power generated by the engine is between the rated power (Cap_{ICE}) and the power at minimum load when the engine is on, while it is zero when the engine is off, as shown in Equation (4), where γ is the ratio of minimum load to rated load.

$$C_{ICE_i,h} = P_{ICE_i,h} m_i + q_i \tag{4}$$

In addition, to prevent wear and tear failures, the motor is constrained not to change state (on or off) more than twice a day, as given in Equation (5) (note that the absolute value can be appropriately treated in order to be included in the problem as linear inequalities).

$$\sum_{h=1}^{23} \left| \delta_{ICE_i,h+1} - \delta_{ICE_i,h} \right| \leq 2 \tag{5}$$

Regarding the DR model, the first requirement to be met is that the integral of the demand associated with the shiftable loads downstream of the DR (subscript DR) is the same as the original demand (subscript $shift$, referring to "shiftable"), as given in Equation (6) (the summations correspond to the integral in the discretization considered).

$$\sum_{h=1}^{24} D_{DR,h} = \sum_{h=1}^{24} D_{shift,h} \tag{6}$$

In addition, the hourly demand cannot be changed more than a certain amount ε (positive or negative) from the original value, as shown by Equation (7).

$$D_{shift,h}(1-\varepsilon) \leq D_{DR,h} \leq D_{shift,h}(1+\varepsilon) \tag{7}$$

The value of ε s varied linearly between 0 and 1 to simulate the degree of user involvement in the DR program (0: zero involvement, 1: maximum involvement).

3.3 Objective function

Equation (8) shows the objective function (f), which represents daily operating costs, where p_{gas} is the specific cost of natural gas, $p_{el,imp}$ the electricity purchasing price from the grid, $p_{el,exp}$ is the selling price and $c_{O\&M}$ is the specific operation and maintenance cost of stationary engines.

$$\begin{aligned} f = \sum_{h=1}^{24} \big[& (C_{ICE_1,h} + C_{ICE_2,h}) p_{gas} + (P_{ICE_1,h} + P_{ICE_2,h}) c_{O\&M} \\ & + P_{imp,h} p_{el,imp,h} - P_{exp,h} p_{el,exp} \big] \end{aligned} \tag{8}$$

Equation 9 calculates the daily CO_2 emissions (φ) attributable to the building, where e_{gas} is the natural gas emission factor and e_{el} is the emission factor of the grid electricity.

$$\varphi = \sum_{h=1}^{24} \left[(C_{ICE_1,h} + C_{ICE_2,h}) e_{gas} + P_{imp,h} e_{el} \right] \tag{9}$$

4 Results

The Gurobi solver in the Python environment has been used to solve the optimization problem. Simulations has been performed in a PC with an Intel(R) Core(TM) i5-7200U processor and 8 GB RAM. The time to compute the solution is less than one-tenth of a second for each simulated combination of input parameters.

4.1 Purchase of electricity at a fixed tariff

Fig. 3 shows the resulting electric power balance for the typical autumn day, obtained by considering the fixed tariff for the purchase of electricity from the grid and zero user involvement in the DR program (ε=0, the modified demand curve downstream of the DR is clearly superimposed on the original demand curve, which is composed of a fixed part, associated with fixed loads, and a variable part, associated with shiftable loads). Production from PV is in slight excess of demand around 12 noon and results in 39 kWh of energy fed into the grid, peaking at 21 kW. The two engines cover most of the remaining demand but operate slightly at rated load. The daily load factor (daily generated energy compared to the energy that would be generated in operation at constant rated power for 24 hours) is 60% for ICE_1, which produces 2867 kWh, and 41% for ICE_2, which produces 976 kWh. Electricity imported from the grid is equal to 147 kWh, with a peak of 63 kW. Overall, 97% of demand is covered by self-generated and self-consumed energy. The daily cost is 760 €, while the CO_2 emissions are 2343 kg.

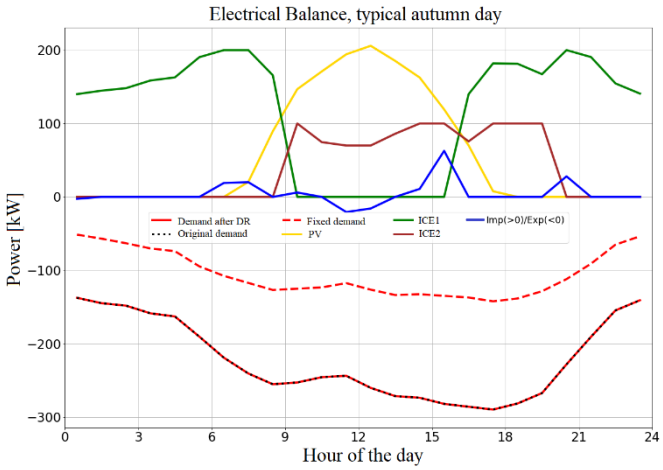

Fig. 3. Electricity balance of the typical autumn day, considering the fixed electricity tariff and ε=0.

Fig. 4 shows the electric power balance obtained considering 50% user involvement in the DR program (ε=0.5). The change in the demand curve, due to the adjustment of shiftable loads, causes the excess generation from PV to be cancelled and all the energy produced to be consumed on-site. The energy fed into the grid is therefore zero. The new demand curve allows ICE_1 to operate for longer at nominal load. It produces 3924 kWh (37% more than the case with zero user involvement), with a load factor of 82%, and remains off only during peak PV production. ICE_2 remains off all the time. The energy imported from the grid is 26 kWh, with a peak power of 12 kW (about one-fifth of the previous case). The daily cost (672 €) drops by 12% compared to the previous case, while CO_2 emissions (2119 kg) drop by

10%, mainly due to the complete on-site utilization of PV-generated energy. Overall, more than 99% of demand is covered by self-generated and self-consumed energy.

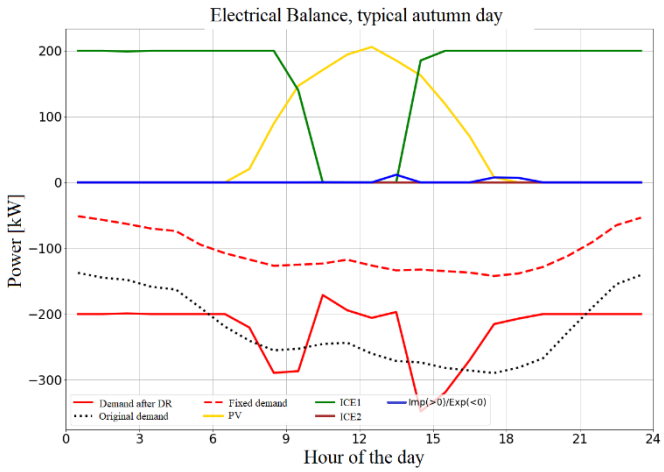

Fig. 4. Electricity balance of the typical autumn day, fixed electricity tariff and ε=0.5.

Fig. 5 shows the trend in costs and emissions as the degree of user involvement (ε) changes for all typical days considered. It can be seen that both costs and emissions drop as involvement increases. However, after an initial rapid decline (between ε=0 and ε=0.5), the rate of cost and emission decline with ε is sharply reduced. Taking summer as an example, costs and emissions drop by 18% from ε=0 to ε=0.5, while they drop by 2% from ε=0.5 to ε=1.

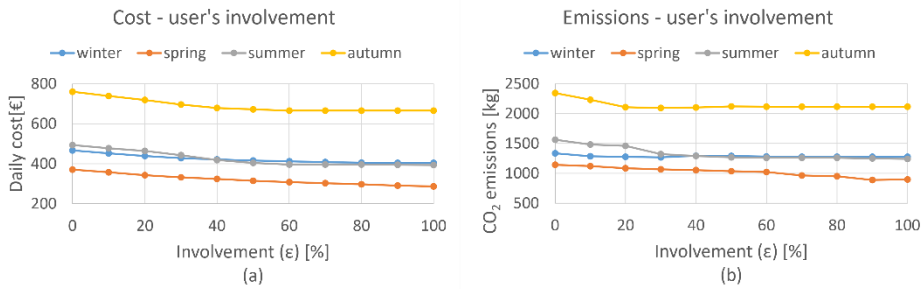

Fig. 5. Daily cost (a) and CO2 emissions (b) as ε changes, fixed electricity tariff.

4.2 Purchase of electricity at variable time-of-use tariff

Fig. 6 shows the electric power balance of the typical autumn day obtained by considering ε=0.5 and the variable tariff for the purchase of electricity from the grid (see Fig. 2). Compared with the case with ε=0.5 and fixed electricity tariff (Fig. 4), two aspects are evident: (i) the energy imported from the grid is much larger and (ii) the energy produced by the engines is less. Starting with the first aspect, it is clear that the lower purchase price of energy from the grid during the nighttime hours makes it convenient to shift consumption during that period. Indeed, the purchase price from the grid turns out to be lower than the generation cost of the engines, which remain off during the night hours. As a result, the energy imported from the grid is equal to 2166 kWh, 83 times more than in the case with

fixed tariff. In addition, the peak withdrawal from the grid turns out to be 265 kW, compared to 12 kW previously. Again, the change in demand means that all the energy produced by PV is consumed locally, cancelling the export of electricity to the grid. Regarding the overall engine generation, there is a 55% decrease, from 3924 kWh to 1785 kWh. ICE_1 has a load factor of 29%, ICE_2 of 17%. Overall, 59% of demand is covered by self-generated and self-consumed energy (40% less than the case with fixed tariff). The effect of variable tariff on daily operating cost is slightly positive. Considering ε=0.5, the daily cost is 660 €, 2% less than the case with fixed tariff. On the other hand, the daily CO_2 emissions are considerably reduced (16%) compared to the fixed-tariff case, dropping to 1776 kg.

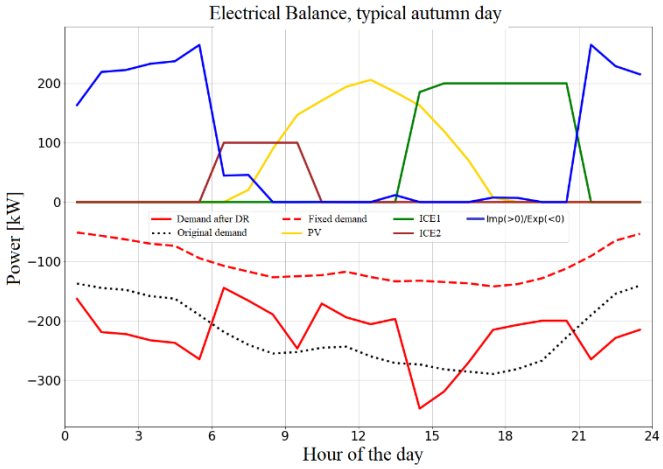

Fig. 6. Electricity balance of the typical autumn day, time-of-use tariff and ε=0.5.

4.3 Comparison of fixed and time-of-use tariffs

As shown in the previous section, the application of the time-of-use tariff results in slightly lower costs and considerably lower emissions compared to the case with a fixed tariff. The proportions remain essentially the same as the user's involvement and the season under consideration change. Fig. 7, on the other hand, shows the differences between fixed and variable tariffs as ε changes in terms of the amount of load shifted through DR and the peak power imported from the grid, which corresponds to the demand peak seen by the grid.

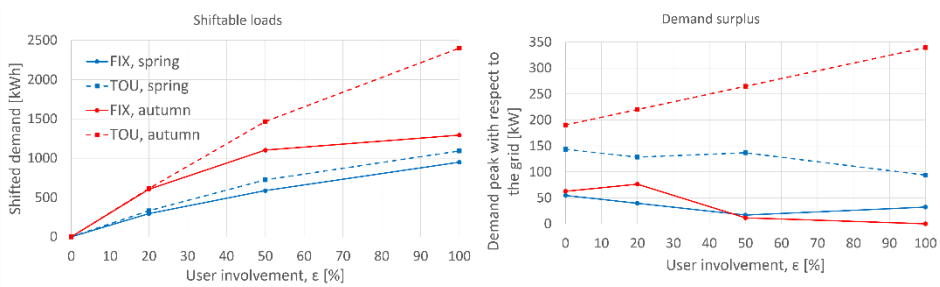

Fig. 7. Comparison of fixed electricity tariff (FIX) and time-of-use tariff (TOU) as ε changes, regarding (a) the amount of demand shifted by the DR and (b) the peak demand seen by the grid.

Clearly, the shifted demand, which is zero for ε=0, increases with ε. However, the increase is greater when considering the variable tariff, which leads to shifting some of the consumption to nighttime hours. For instance, considering autumn and ε=0.5, the demand shifted considering the variable tariff is equal to 1465 kWh, compared to 1102 kWh obtained with fixed tariff (25% less). Thus, the variable tariff requires more user effort in load management.

The peak demand seen from the grid also appears to be higher considering the variable tariff. This is indicative of a worse balance at the building level between demand and generation, which is in turn due to the lower contribution of stationary engines in meeting demand. Considering autumn, the difference between the two tariffs also tends to diverge. The peak recorded with variable tariff exceeds that recorded with fixed tariff by 128 kW for ε=0 and by 339 kW for ε=1.

5 Conclusions

By setting up and solving an optimization problem, the paper has evaluated the energy, economic, and environmental benefits that demand response (DR) can provide at the building level. A tourist facility located in central Germany that includes several electrical loads, some of which have been identified as suitable for DR, has been considered as a case study. The total electrical demand of the facility is partially covered by a photovoltaic plant and two stationary gas-fired internal combustion engines.

First and foremost, the application of DR leads to increasing the share of PV-generated energy that is consumed on-site, up to full self-consumption after a threshold level of user flexibility depending on the seasonal typical day considered. This corresponds to zeroing the electricity fed into the grid (back-flow), which can be a cause of grid instability.

Increased self-consumption from PV also has a twofold positive effect: on the one hand, it reduces the daily costs of meeting electricity demand, as less energy is drawn from the grid; on the other hand, it reduces carbon dioxide emissions attributable to the building. Considering the application of DR to 50% of the consumption of the suitable loads, it is possible to reduce costs by 12% and emissions by 10%. This is partly due also to greater use of stationary engines at rated load, thus with lower specific consumption.

These benefits are even greater when a variable time-of-use electricity purchase tariff is applied. Indeed, an additional 2% reduction in costs and 16% reduction in emissions can be achieved compared to a fixed-price tariff. However, the currently available time-of-use tariffs propose lowered prices during nighttime hours, which are typically off-peak in terms of electricity demand. This causes much of the DR-eligible consumption to be shifted to those very hours, while also reducing the less cost-effective engine generation. Therefore, this increases the energy imported from the grid, which is the cause of new peak demand.

It is therefore clear that, from a strictly economic and environmental point of view, the choice of variable time-of-use tariff is the optimal solution for the customer. However, from a system perspective, it makes the building more dependent on the grid.

Looking ahead, the application of hourly tariffs indexed to electricity prices in the wholesale market, which better represent market dynamics, is expected to be analysed. It is possible that this will reduce the problems associated with peak demand.

In addition, it is planned to include building thermal demand in the study, with a twofold objective: first, to consider the cogeneration potential of stationary engines, and second, to extend the DR to building heating.

Finally, to make the proposed model more easily implementable, it will be important to identify targeted DR strategies depending on the type of load considered.

References

1. E. Papadis and G. Tsatsaronis, Challenges in the decarbonization of the energy sector. Energy. **205**, 118025, (2020). https://doi.org/10.1016/j.energy.2020.118025
2. Eurostat, Energy statistics - an overview. (2023). https://ec.europa.eu/eurostat/statistics-explained/index.php?title=Energy_statistics_-_an_overview
3. European Union, A European Green Deal. (2023). https://ec.europa.eu/info/strategy/priorities-2019-2024/european-green-deal_en
4. M. A. Zehir, A. Batman, and M. Bagriyanik, Review and comparison of demand response options for more effective use of renewable energy at consumer level. Renewable and Sustainable Energy Reviews. **56**, 631-642, (2016). https://doi.org/10.1016/j.rser.2015.11.082
5. G. Chantzis, E. Giama, S. Nižetić, and A. M. Papadopoulos, The potential of demand response as a tool for decarbonization in the energy transition. Energy and Buildings. **296**, 113255, (2023). https://doi.org/10.1016/j.enbuild.2023.113255
6. U.S. Department of Energy, "Benefits of Demand Response in Electricity Markets and Reccomandations for Achieving them - A Report to the United States Congress Pursuant to Section 1252 of the Energy Policy Act of 2005," 2006.
7. P. Bradley, M. Leach, and J. Torriti, A review of the costs and benefits of demand response for electricity in the UK. Energy Policy. **52**, 312-327, (2013). https://doi.org/10.1016/j.enpol.2012.09.039
8. M. H. Albadi and E. F. El-Saadany, A summary of demand response in electricity markets. Electric Power Systems Research. **78**, 1989-1996, (2008). https://doi.org/10.1016/j.epsr.2008.04.002
9. N. Good, K. A. Ellis, and P. Mancarella, Review and classification of barriers and enablers of demand response in the smart grid. Renewable and Sustainable Energy Reviews. **72**, 57-72, (2017). https://doi.org/10.1016/j.rser.2017.01.043
10. J. Torriti, M. G. Hassan, and M. Leach, Demand response experience in Europe: Policies, programmes and implementation. Energy. **35**, 1575-1583, (2010). https://doi.org/10.1016/j.energy.2009.05.021
11. Q. Wang, C. Zhang, Y. Ding, G. Xydis, J. Wang, and J. Østergaard, Review of real-time electricity markets for integrating Distributed Energy Resources and Demand Response. Applied Energy. **138**, 695-706, (2015). https://doi.org/10.1016/j.apenergy.2014.10.048
12. M. H. Imani, M. J. Ghadi, S. Ghavidel, and L. Li, Demand Response Modeling in Microgrid Operation: a Review and Application for Incentive-Based and Time-Based Programs. Renewable and Sustainable Energy Reviews. **94**, 486-499, (2018). https://doi.org/10.1016/j.rser.2018.06.017
13. F. Shariatzadeh, P. Mandal, and A. K. Srivastava, Demand response for sustainable energy systems: A review, application and implementation strategy. Renewable and Sustainable Energy Reviews. **45**, 343-350, (2015). https://doi.org/10.1016/j.rser.2015.01.062
14. H. T. Haider, O. H. See, and W. Elmenreich, A review of residential demand response of smart grid. Renewable and Sustainable Energy Reviews. **59**, 166-178, (2016). https://doi.org/10.1016/j.rser.2016.01.016

15. I. Hussain, S. Mohsin, A. Basit, Z. A. Khan, U. Qasim, and N. Javaid, A Review on Demand Response: Pricing, Optimization, and Appliance Scheduling. Procedia Computer Science. **52**, 843-850, (2015). https://doi.org/10.1016/j.procs.2015.05.141
16. F. Babonneau, M. Caramanis, and A. Haurie, A linear programming model for power distribution with demand response and variable renewable energy. Applied Energy. **181**, 83-95, (2016). https://doi.org/10.1016/j.apenergy.2016.08.028
17. A. Rafinia, J. Moshtagh, and N. Rezaei, Towards an enhanced power system sustainability: An MILP under-frequency load shedding scheme considering demand response resources. Sustainable Cities and Society. **59**, 102168, (2020). https://doi.org/10.1016/j.scs.2020.102168
18. M. Tostado-Véliz, A. A. Ghadimi, M. R. Miveh, D. Sánchez-Lozano, A. Escamez, and F. Jurado, A Novel Stochastic Mixed-Integer-Linear-Logical Programming Model for Optimal Coordination of Hybrid Storage Systems in Isolated Microgrids Considering Demand Response. Batteries. **8**, (2022). 10.3390/batteries8110198
19. E. Dal Cin, G. Carraro, G. Volpato, A. Lazzaretto, and P. Danieli, A multi-criteria approach to optimize the design-operation of Energy Communities considering economic-environmental objectives and demand side management. Energy Conversion and Management. **263**, 115677, (2022). https://doi.org/10.1016/j.enconman.2022.115677
20. G. Volpato, G. Carraro, M. Cont, P. Danieli, S. Rech, and A. Lazzaretto, General guidelines for the optimal economic aggregation of prosumers in energy communities. Energy. **258**, 124800, (2022). https://doi.org/10.1016/j.energy.2022.124800
21. C. Henggeler Antunes, M. J. Alves, and I. Soares, A comprehensive and modular set of appliance operation MILP models for demand response optimization. Applied Energy. **320**, 119142, (2022). https://doi.org/10.1016/j.apenergy.2022.119142
22. H. T. Dinh, K.-h. Lee, and D. Kim, Supervised-learning-based hour-ahead demand response for a behavior-based home energy management system approximating MILP optimization. Applied Energy. **321**, 119382, (2022). https://doi.org/10.1016/j.apenergy.2022.119382
23. Veil Energy, e.boost. (2024). https://veil-energy.eu/prodotti/eem/
24. Y. Wang, Y. Ma, F. Song, Y. Ma, C. Qi, F. Huang, *et al.*, Economic and efficient multi-objective operation optimization of integrated energy system considering electro-thermal demand response. Energy. **205**, 118022, (2020). https://doi.org/10.1016/j.energy.2020.118022
25. European Commission, Photovoltaic Geographical Information System (PVGIS). (2024). https://re.jrc.ec.europa.eu/pvg_tools/it/#MR
26. DESTATIS - Statisches Bundesmat, Data on energy price trends - Long-time series to Dezember 2022. (2023). https://www.destatis.de/EN/Themes/Economy/Prices/Publications/Downloads-Energy-Price-Trends/energy-price-trends-pdf-5619002.html
27. J. Stute and M. Kühnbach, Dynamic pricing and the flexible consumer – Investigating grid and financial implications: A case study for Germany. Energy Strategy Reviews. **45**, 100987, (2023). https://doi.org/10.1016/j.esr.2022.100987
28. Electricity Maps, Emissioni di CO2 in tempo reale del consumo elettrico. (2023). https://app.electricitymaps.com/map
29. SMARD - Bundesnetzagentur, Market data. (2023). https://www.smard.de/en

30. Danish Energy Agency, Technology Data. (2023). https://ens.dk/en/our-services/projections-and-models/technology-data
31. P. Sterchele, J. Brandes, J. Heilig, D. Wrede, C. Kost, T. Schlegl*, et al.*, "Paths to a Climate-Neutral Energy System. The German Energy Transition in its Social Context," Fraunhofer ISE2020. https://www.ise.fraunhofer.de/en/publications/studies/paths-to-a-climate-neutral-energy-system.html
32. S. Rech, Smart Energy Systems: Guidelines for Modelling and Optimizing a Fleet of Units of Different Configurations. Energies. **12**, 1320, (2019). doi:10.3390/en12071320